On the Influence of a Wire placed Upstream of a Rotating Cylinder: Three-dimensional effects

A. Rao[1], A. Radi[1], J. S. Leontini[2], M. C. Thompson[1], J. Sheridan[1] and K. Hourigan[1,3]

[1]Fluids Laboratory for Aeronautical and Industrial Research (FLAIR),
Department of Mechanical and Aerospace Engineering, Monash University, VIC, 3800, Australia

[2]Department of Mechanical Engineering and Product Design Engineering,
Swinburne University of Technology, John St, Hawthorn 3162, Australia

[3]Division of Biological Engineering, Faculty of Engineering,
Monash University, VIC, 3800, Australia

Abstract

Recent experimental investigations [12] on the three-dimensionality of the wake of a rotating cylinder at low Reynolds numbers showed the onset of a subharmonic mode, (Mode C), at rotation rates lower that that predicted by the linear stability analysis of [13]. For the experimental flow visualisation of the wake, hydrogen bubbles were generated from a platinum wire upstream of the rotating cylinder and illuminated by a laser sheet. The influence of the wire is investigated here by modelling the platinum wire as a circular cylinder, whose diameter is one-fiftieth of that of the rotating cylinder. Linear stability analysis is performed to investigate the three-dimensional stability. An asymmetry in the wake occurs when the wire is upstream and above the cylinder, leading to the growth of the subharmonic mode, at much lower rotation rates compared to the case without the wire.

Introduction

The flow past a rotating circular cylinder in freestream has been widely investigated by several researchers [2, 4, 8, 9] and has garnered much attention recently [1, 10, 11, 12, 13, 14, 16]. The flow past the cylinder depends on two non-dimensional parameters; the flow Reynolds number, Re, $Re = UD/\nu$, where U is the inflow velocity, D is the cylinder diameter and ν is the kinematic viscosity of the fluid. The second parameter is the non-dimensionalised rotation rate, α, which is the ratio of the surface velocity to the inflow velocity and is given by $\alpha = \omega D/2U$, where ω is the angular velocity of the cylinder.

At low rotation rates, the flow past the rotating cylinder closely resembles that of the non-rotating cylinder; that is the flow transitions from steady to unsteady flow around $Re \simeq 46$, followed by the transition to three-dimensional mode via *mode A* instability around $Re \simeq 190$, followed by the transition to *mode B* instability around $Re \simeq 260$ [3, 27, 28]. The spanwise wavelength of the mode A instability is $\simeq 4D$ while that of mode B is $\simeq 0.8D$. As the rotation rate is increased, the onset of unsteady flow is delayed to higher Reynolds numbers and is suppressed for $\alpha \gtrsim 2$ [4, 9]. The onset of three-dimensional flow at other Reynolds numbers had not been investigated until recently. Three-dimensional Direct Numerical Simulations (DNS) performed by [1] for $\alpha \leqslant 1.5$, showed that the onset of three-dimensionality was delayed to $Re \simeq 220$ for $\alpha = 0.5$.

Comprehensive numerical investigations using linear stability analysis were performed by [13, 16] to map the various three-dimensional modes that are observed for $\alpha \leqslant 2.5, Re \leqslant 350$. They observed that the onset of mode A and mode B instabilities was delayed to higher Reynolds numbers as the rotation rate is increased to $\alpha \simeq 1.9$. Furthermore, they observed a subharmonic mode for $1.5 \lesssim \alpha \lesssim 1.85$ to be the first three-dimensional mode to be unstable to spanwise perturbations with spanwise wavelengths in-between that of modes A and B. This subharmonic mode, *mode C*, was previously observed when the flow asymmetry was broken such as in the wake behind rings [22, 23], inclined square cylinders [20, 21] and in the wake of a non-rotating cylinder when destabilised by a trip wire placed downstream of the cylinder [30, 31].

Recent experimental investigations by [12] confirmed the three-dimensional modes reported by [13]. However, mode C was observed to occur at much lower rotation rates than that reported in the linear stability analysis of [13]. At $Re = 275$, for $0.5 \lesssim \alpha \lesssim 0.7$, mode C was observed alongside mode B, and for $1 \lesssim \alpha \lesssim 1.7$, mode C was the single dominant mode. It was further observed that the spanwise wavelength of mode C decreased as the rotation rate was increased from $\alpha = 0.5$ to $\alpha \simeq 1.8$. Notably, they used a platinum wire for the generation of the hydrogen bubbles, which were then illuminated by a thin laser sheet to visualise the wake behind the cylinder. This wire (of diameter one-hundredth of the cylinder) was placed approximately five cylinder diameters upstream and one diameter above the rotating cylinder. Figure 1 shows the experimental flow visualisation of the mode C instability at $\alpha = 1, Re = 275$, when the wire is placed upstream of the cylinder. Clearly, spanwise vortices are shifted by half a wavelength every period, demonstrating the subharmonic nature of this mode.

The studies of [29, 30, 31] have also shown that a subharmonic mode can be triggered by placing a trip wire in the wake of a non-rotating cylinder, leading to the suppression of the natural state of the wake, where mode A is traditionally observed. It is thus hypothesised that the location of the platinum wire at a distance of five cylinder diameters (or, 500 wire diameters) destabilises the wake, altering the critical onset of the three-dimensional modes of the rotating cylinder. To test this hypothesis, numerical modelling including the wire was undertaken, with the wire being modelled as a circular cylinder one-fiftieth the diameter of the rotating cylinder ($d/D = 50$, where d is the diameter of the wire). Note that the wire diameter is twice that used in the experiments. This is to ameliorate the restriction on the time-step caused by small elements in the vicinity of the wire.

The remainder of this paper is organised as follows; the following section briefly details the experimental and numerical setup, following which the results are presented. This is followed by conclusions.

Numerical and experimental setup

The Navier-Stokes equations are solved in two- and three-dimensions using a spectral element formulation. The computational domain consists of quadrilateral elements which are concentrated in the vicinity of the two cylinders to accurately capture the velocity gradients. These quadrilateral elements

(a) $t = t_0$

(b) $t = t_0 + T$
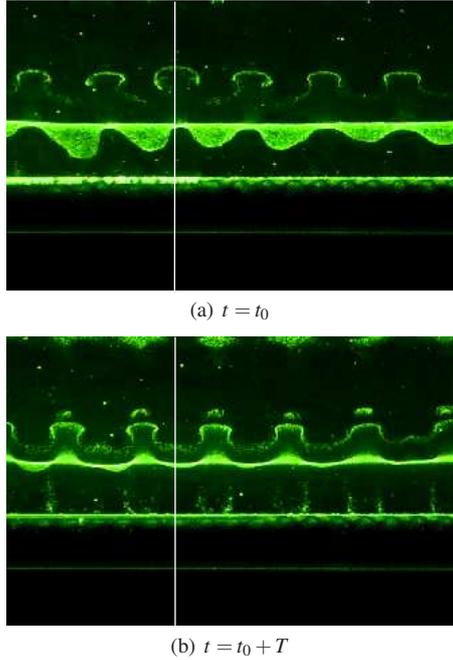
Figure 1: Experimental flow visualisation at $\alpha = 1, Re = 275$, showing the mode C instability for a cylinder of spanwise distance of $\simeq 8D$ over one consecutive period. The white guidelines drawn at the spatial location shows the spanwise shift the vortices by half a wavelength. The wire is upstream of the cylinder and not shown in these images. Flow is from bottom to top in both these images.

(a) $t = t_0$

(b) $t = t_0 + T$

Figure 2: Visualisation of the spanwise perturbation vorticity contours at $\alpha = 0.5, Re = 280, \lambda/D = 1.6$ over two consecutive periods. Perturbation contours are between levels $\pm 0.1 D/U$ and are shown by red/blue colouring. These are overlaid with continuous lines which indicate base flow vorticity contours between $\pm 0.275 D/U$. Flow is from left to right in these images.

were further subdivided into internal node points, which were distributed according to Gauss-Legendre-Lobatto quadrature points. The velocity and pressure fields are represented by tensor products of Lagrangian polynomial interpolants. Spectral convergence is achieved as the polynomial order is increased [5]. The number of node points within each element $(N \times N)$ can be specified at runtime with the interpolating polynomial order in each direction being $N - 1$. A second-order fractional time-stepping technique is used to sequentially integrate the advection, pressure and diffusion terms of the Navier-Stokes equations forward in time. More details of the time-stepping scheme can be found in [26].

To investigate the stability of the flow to three-dimensional perturbations, stability analysis is carried out over a small range of the parameter space to compare with the experimental setup. The Navier-Stokes equations are linearised and the spanwise wavelengths are constructed as a set of Fourier modes. These equations are integrated forward in time and the growth of these perturbations is monitored. After several time periods, the fastest growing modes dominate the system. The growth rate (σ) of the stability multiplier is then computed; for $\sigma < 0$, the perturbations decay and for $\sigma > 0$, the perturbations grow and the flow transitions to three-dimensionality. More details on this method has can be found in [6, 13, 15, 17, 18, 19, 22, 24, 25].

The experimental setup consisted of a stiff carbon-fibre cylinder of 5.8mm diameter driven by a stepper motor in the FLAIR open surface water channel. The wetted length of the cylinder in the channel was approximately 130 times the cylinder diameter. The cylinder wobbling was kept within 2.5% of the cylinder diameter even for high rotation rates of $\alpha = 5$. This is within acceptable limits to not unduly influence the flow behaviour [7].
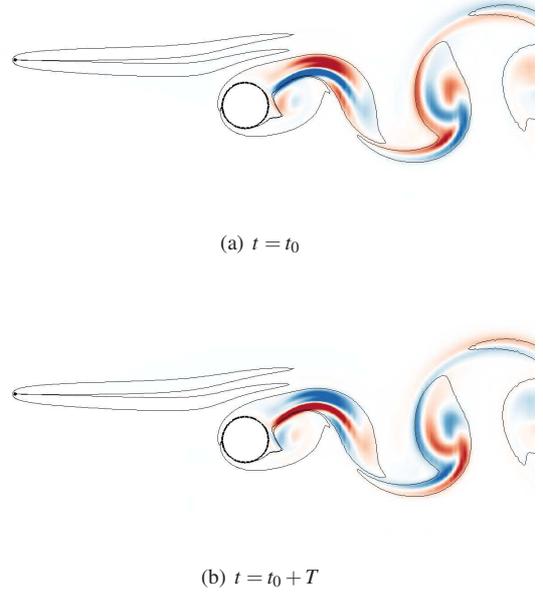
A platinum wire (50μm) positioned five cylinder diameters upstream and parallel to the main cylinder axis was used for the generation of a sheet of hydrogen bubbles. The sheet passed the rotating cylinder and was entrained by the near wake, making the three-dimensional structures visible. A continuous laser sheet was used for illumination. The images were recorded with a digital camera and numerically processed to extract information on wavelengths and mode symmetries. More details on the experimental setup are described in [12].

Results

The flow past a rotating cylinder (centred at $(x_0, y_0) = (0, 0)$) with a wire upstream (at $(x, y) = (-5, 1)$) is presented here for $\alpha \leqslant 2, Re \leqslant 400$. The boundaries of the computational domain were placed in excess of $50D$ from the cylinder to prevent significant blockage effects. To check if the mesh was sufficiently refined to capture the flow at the highest rotation rate, spatial resolution studies was carried out between $N = 4$ to $N = 11$. For a resolution of $N = 7$, the force-coefficients and shedding frequency were well within 0.5% of the values at the highest resolution. Additionally, the spatial resolution tests were carried out at $\alpha = 1.5, Re = 280$ to confirm that a resolution of $N = 7$ was sufficient to capture the growth rate of the fastest growing mode. Hence, this resolution was chosen for the rest of the computations.

As the rotation rate is increased from $\alpha = 0$, the first instance of mode C instability is observed at $\alpha = 0.5$. Shown in figure 2 are the spanwise perturbation vorticity contours at $\alpha = 0.5, Re = 280, \lambda/D = 1.6$ over two consecutive periods. The perturbation fields alternate each period, indicating the subharmonic nature of mode C [6, 22, 23]. The asymmetry of the wake can be attributed not only to the rotation of the cylinder, but also to the wake from the wire, whose influence extends $250d$ downstream.
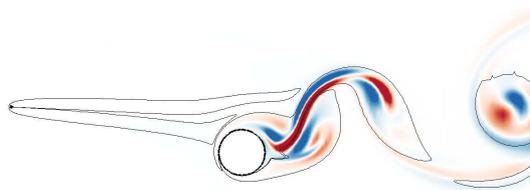
(a) $\alpha = 1.25, \lambda/D = 1.4$
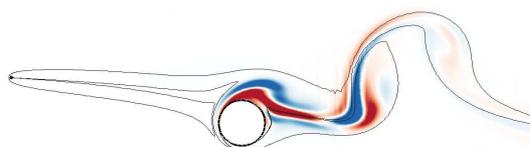
(b) $\alpha = 1.70, \lambda/D = 1.5$

Figure 3: Visualisation of the spanwise perturbation vorticity contours at the specified parameters at $Re = 280$. Contour shading as per figure 2. Flow is from left to right in these images.

On increasing the rotation rate, mode C is observed until $\alpha \simeq 1.7$. As the magnitude of rotation increases, the wake of the wire upstream is drawn downwards, which further leads to the distortion in the already asymmetric wake. Shown in figure 3 are the spanwise perturbation contours at the specified rotation rates.

Figure 4 shows the comparison between the experimentally observed spanwise wavelength of the mode C instability with rotation rate at $Re = 275$ [12] and the numerically computed values of spanwise wavelength at the maximum growth rate from the stability analysis at $Re = 280$. The numerical values are in good agreement with the experimental counterparts over the entire range.

A stand-alone three-dimensional simulation was undertaken at $\alpha = 1, Re = 280$. As spanwise distance of $z/D = 8$ with 64 Fourier planes was chosen to capture five instances of the mode
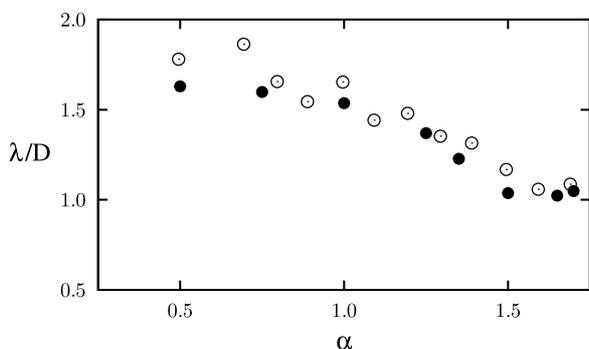
Figure 4: Comparison between the spanwise wavelengths with rotation rate for $Re \simeq 280$. The filled circles ($\bullet$) are from the numerical simulations, while the open circles ($\circ$) are from the experimental investigations of [12].
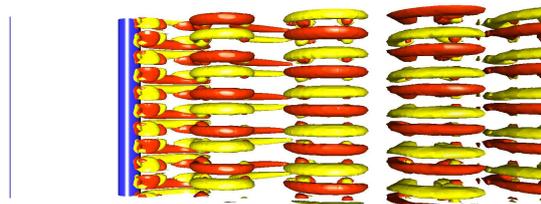
Figure 5: Visualisation of the streamwise vorticity isosurfaces (red and yellow) for the flow past a rotating cylinder (in blue) at $\alpha = 1, Re = 280$ over a spanwise distance of $z/D = 8$. The wire can be seen at the far left of the image. The flow is from left to right.

C instability. Shown in figure 5 are the streamwise vorticity isosurfaces of the saturated wake. The vortices are shifted by half a wavelength every consecutive row, indicating the subharmonic nature of the wake, which has been triggered by the wire, while the natural state of the wake without the wire is mode A (not shown). This compares well with the experimental image shown in figure 1.

Conclusions

Flow past a rotating cylinder with a wire upstream was investigated for $\alpha \leqslant 2, Re \leqslant 400$. When the wire was placed upstream and above the cylinder, the flow transitions to a subharmonic three-dimensional mode (mode C) at lower rotation rates than without the wire. While modes A and mode B instabilities are resilient to the location of the wire, mode C is triggered for $\alpha \gtrsim 0.5$. These simulations also explain the premature onset of mode C instability in the experimental investigations of [12].

The results clearly indicate that even 500 diameters downstream, the remaining wake from the visualisation wire is still sufficient to significantly influence wake transitions. This once again serves as a warning about the use of intrusive methods for observing/quantifying flows, even when they seem to be effectively non-intrusive.

References

[1] Akoury, R. E., Braza, M., Perrin, R., Harran, G. and Hoarau, Y., The three-dimensional transition in the flow around a rotating cylinder, *Journal of Fluid Mechanics*, **607**, 2008, 1–11.

[2] Badr, H. M., Coutanceau, M., Dennis, S. C. R. and Menard, C., Unsteady flow past a rotating circular cylinder at Reynolds numbers 10^3 and 10^4, *Journal of Fluid Mechanics*, **220**, 1990, 459–484.

[3] Barkley, D. and Henderson, R. D., Three-dimensional Floquet stability analysis of the wake of a circular cylinder,

Journal of Fluid Mechanics, **322**, 1996, 215–241.

[4] Kang, S., Choi, H. and Lee, S., Laminar flow past a rotating circular cylinder, *Physics of Fluids*, **11**, 1999, 3312–3321.

[5] Karniadakis, G. E. and Sherwin, S. J., *Spectral/hp Methods for Computational Fluid Dynamics*, Oxford University Press, Oxford, 2005.

[6] Leontini, J. S., Thompson, M. C. and Hourigan, K., Three-dimensional transition in the wake of a transversely oscillating cylinder, *Journal of Fluid Mechanics*, **577**, 2007, 79–104.

[7] Mittal, S., Flow past rotating cylinders: Effect of eccentricity, *Journal of Applied Mechanics*, **68**, 2001, 543–552.

[8] Mittal, S., Three-dimensional instabilities in flow past a rotating cylinder, *Journal of Applied Mechanics*, **71**, 2004, 89–95.

[9] Mittal, S. and Kumar, B., Flow past a rotating cylinder, *Journal of Fluid Mechanics*, **476**, 2003, 303–334.

[10] Pralits, J. O., Brandt, L. and Giannetti, F., Instability and sensitivity of the flow around a rotating circular cylinder, *Journal of Fluid Mechanics*, **650**, 2010, 513–536.

[11] Pralits, J. O., Giannetti, F. and Brandt, L., Three-dimensional instability of the flow around a rotating circular cylinder, *Journal of Fluid Mechanics*, **730**, 2013, 5–18.

[12] Radi, A., Thompson, M. C., Rao, A., Hourigan, K. and Sheridan, J., Experimental evidence of new three-dimensional modes in the wake of a rotating cylinder, *Journal of Fluid Mechanics*, **734**, 2013, 567–594.

[13] Rao, A., Leontini, J., Thompson, M. C. and Hourigan, K., Three-dimensionality in the wake of a rotating cylinder in a uniform flow, *Journal of Fluid Mechanics*, **717**, 2013, 1–29.

[14] Rao, A., Leontini, J. S., Thompson, M. C. and Hourigan, K., Three-dimensionality in the wake of a rapidly rotating cylinder in uniform flow, *Journal of Fluid Mechanics*, **730**, 2013, 379–391.

[15] Rao, A., Passaggia, P.-Y., Bolnot, H., Thompson, M. C., Leweke, T. and Hourigan, K., Transition to chaos in the wake of a rolling sphere, *Journal of Fluid Mechanics*, **695**, 2012, 135–148.

[16] Rao, A., Radi, A., Leontini, J. S., Thompson, M. C., Sheridan, J. and Hourigan, K., A review of rotating cylinder wake transitions, *Journal of Fluids and Structures*, available online.

[17] Rao, A., Stewart, B. E., Thompson, M. C., Leweke, T. and Hourigan, K., Flows past rotating cylinders next to a wall, *Journal of Fluids and Structures*, **27**, 2011, 668 – 679.

[18] Rao, A., Thompson, M. C., Leweke, T. and Hourigan, K., The flow past a circular cylinder translating at different heights above a wall, *Journal of Fluids and Structures*, **41**, 2013, 9–21, special issue on Bluff Body Flows (Blubof2011).

[19] Ryan, K., Thompson, M. C. and Hourigan, K., Three-dimensional transition in the wake of elongated bluff bodies, *Journal of Fluid Mechanics*, **538**, 2005, 1–29.

[20] Sheard, G. J., Wake stability features behind a square cylinder: Focus on small incidence angles, *Journal of Fluids and Structures*, **27**, 2011, 734 – 742.

[21] Sheard, G. J., Fitzgerald, M. J. and Ryan, K., Cylinders with square cross-section: wake instabilities with incidence angle variation, *Journal of Fluid Mechanics*, **630**, 2009, 43–69.

[22] Sheard, G. J., Thompson, M. C. and Hourigan, K., From spheres to circular cylinders: non-axisymmetric transitions in the flow past rings, *Journal of Fluid Mechanics*, **506**, 2004, 45–78.

[23] Sheard, G. J., Thompson, M. C. and Hourigan, K., Sub-harmonic mechanism of the mode C instability, *Physics of Fluids*, **17**, 2005, 1–4.

[24] Stewart, B. E., Hourigan, K., Thompson, M. C. and Leweke, T., Flow dynamics and forces associated with a cylinder rolling along a wall, *Physics of Fluids*, **18**, 2006, 111701–1–111701–4.

[25] Stewart, B. E., Thompson, M. C., Leweke, T. and Hourigan, K., The wake behind a cylinder rolling on a wall at varying rotation rates, *Journal of Fluid Mechanics*, **648**, 2010, 225–256.

[26] Thompson, M. C., Hourigan, K., Cheung, A. and Leweke, T., Hydrodynamics of a particle impact on a wall, *Applied Mathematical Modelling*, **30**, 2006, 1356–1369.

[27] Williamson, C. H. K., The existence of two stages in the transition to three-dimensionality of a cylinder wake, *Physics of Fluids*, **31**, 1988, 3165–3168.

[28] Williamson, C. H. K., Vortex dynamics in the cylinder wake, *Annual Review of Fluid Mechanics*, **28**, 1996, 477–539.

[29] Yildirim, I., Rindt, C. C. M. and van Steenhoven, A. A., Energy contents and vortex dynamics in Mode-C transition of wired-cylinder wake, *Physics of Fluids*, **25**.

[30] Yildirim, I., Rindt, C. C. M. and van Steenhoven, A. A., Mode c flow transition behind a circular cylinder with a near-wake wire disturbance, *Journal of Fluid Mechanics*, **727**, 2013, 30–55.

[31] Zhang, H., Fey, U., Noack, B. R., Konig, M. and Eckelemann, H., On the transition of the cylinder wake, *Physics of Fluids*, **7**, 1995, 779–794.